Gastroenterology 2016;150:477–487

Association Between Response to Etrolizumab and Expression of Integrin αE and Granzyme A in Colon Biopsies of Patients With Ulcerative Colitis

Gaik W. Tew,[1] Jason A. Hackney,[1] Deena Gibbons,[2] Christopher A. Lamb,[3] Diana Luca,[1] Jackson G. Egen,[1] Lauri Diehl,[1] Jeff Eastham Anderson,[1] Severine Vermeire,[4] John C. Mansfield,[3] Brian G. Feagan,[5] Julian Panes,[6] Daniel C. Baumgart,[7] Stefan Schreiber,[8] Iris Dotan,[9] William J. Sandborn,[10] John A. Kirby,[3] Peter M. Irving,[2] Gert De Hertogh,[4] Gert A. Van Assche,[4,11] Paul Rutgeerts,[4] Sharon O'Byrne,[1] Adrian Hayday,[2] and Mary E. Keir[1]

[1]Genentech Research and Early Development, South San Francisco, California; [2]King's College, London, United Kingdom; [3]Newcastle University, Newcastle upon Tyne, United Kingdom; [4]University of Leuven, Leuven, Belgium; [5]University of Western Ontario, London, Ontario, Canada; [6]Hospital Clinic de Barcelona, Institut d'Investigacions Biomèdiques August Pi i Sunyer, Centro de Investigación Biomédica en Red de Enfermedades Hepáticas y Digestivas, Barcelona, Spain; [7]Charité Medical School, Humboldt-University of Berlin, Germany; [8]Department of Medicine I, University Hospital Schleswig-Holstein, Christian Albrechts University, Kiel, Germany; [9]Inflammatory Bowel Disease Center, Department of Gastroenterology and Liver Diseases, Tel Aviv Medical Center and Sackler Faculty of Medicine, Tel Aviv, Israel; [10]University of California San Diego, La Jolla, California; and [11]University of Toronto, Toronto, Ontario, Canada

BACKGROUND & AIMS: Etrolizumab is a humanized monoclonal antibody against the β7 integrin subunit that has shown efficacy vs placebo in patients with moderate to severely active ulcerative colitis (UC). Patients with colon tissues that expressed high levels of the integrin αE gene (*ITGAE*) appeared to have the best response. We compared differences in colonic expression of *ITGAE* and other genes between patients who achieved clinical remission with etrolizumab vs those who did. **METHODS:** We performed a retrospective analysis of data collected from 110 patients with UC who participated in a phase 2 placebo-controlled trial of etrolizumab, as well as from 21 patients with UC or without inflammatory bowel disease (controls) enrolled in an observational study at a separate site. Colon biopsies were collected from patients in both studies and analyzed by immunohistochemistry and gene expression profiling. Mononuclear cells were isolated and analyzed by flow cytometry. We identified biomarkers associated with response to etrolizumab. In the placebo-controlled trial, clinical remission was defined as total Mayo Clinic Score ≤2, with no individual subscore >1, and mucosal healing was defined as endoscopic score ≤1. **RESULTS:** Colon tissues collected at baseline from patients who had a clinical response to etrolizumab expressed higher levels of T-cell–associated genes than patients who did not respond ($P < .05$). Colonic $CD4^+$ integrin αE^+ cells from patients with UC expressed higher levels of granzyme A messenger RNA (*GZMA* mRNA) than $CD4^+$ αE^- cells ($P < .0001$); granzyme A and integrin αE protein were detected in the same cells. Of patients receiving 100 mg etrolizumab, a higher proportion of those with high levels of *GZMA* mRNA (41%) or *ITGAE* mRNA (38%) than those with low levels of *GZMA* (6%) or *ITGAE* mRNA (13%) achieved clinical remission ($P < .05$) and mucosal healing (41% $GZMA^{high}$ vs 19% $GZMA^{low}$ and 44% $ITGAE^{high}$ vs 19% $ITGAE^{low}$). Compared with $ITGAE^{low}$ and $GZMA^{low}$ patients, patients with $ITGAE^{high}$ and $GZMA^{high}$ had higher baseline numbers of epithelial crypt-associated integrin αE^+ cells ($P < .01$ for both), but a smaller number of crypt-associated integrin αE^+ cells after etrolizumab treatment ($P < .05$ for both). After 10 weeks of etrolizumab treatment, expression of genes associated with T-cell activation and genes encoding inflammatory cytokines decreased by 40%–80% from baseline ($P < .05$) in patients with colon tissues expressing high levels of *GZMA* at baseline. **CONCLUSIONS:** Levels of *GZMA* and *ITGAE* mRNAs in colon tissues can identify patients with UC who are most likely to benefit from etrolizumab; expression levels decrease with etrolizumab administration in $biomarker^{high}$ patients. Larger, prospective studies of markers are needed to assess their clinical value.

Keywords: IBD Drug; Response to Therapy; Anti-Integrin; Personalized Medicine.

Ulcerative colitis (UC) is a chronic inflammatory disease of the colon. Current therapies, such as corticosteroids, immunosuppressants, and anti–tumor necrosis factor (TNF) antibodies, are not universally effective at induction and maintenance of remission,[1] with ≈25% of patients requiring colectomy.[2] This variable response to treatment and disease progression may reflect significant heterogeneity in disease pathobiology.[3,4] Improved stratification driven by patient heterogeneity may help guide choice of therapeutic intervention and enhance efficacy and safety.

The integrin-dependent migration and retention of leukocytes to the gut plays an important role in the pathogenesis

Abbreviations used in this paper: **DC, dendritic cell; IEL, intraepithelial lymphocyte; IL, interleukin; LP, lamina propria; MAdCAM-1, mucosal vascular addressin cell adhesion molecule 1; NK, natural killer; qPCR, quantitative polymerase chain reaction; TNF, tumor necrosis factor; UC, ulcerative colitis.**

Most current article

0016-5085
http://dx.doi.org/10.1053/j.gastro.2015.10.041

of inflammatory bowel disease (IBD).[5,6] Subsets of immune cells, including B cells, naïve and gut homing T cells, natural killer (NK) cells, dendritic cells, stimulated macrophages, monocytes, and eosinophils[7] express $\alpha4\beta7$ to mediate binding to mucosal addressin cell adhesion molecule 1 (MAdCAM-1) on high endothelial venules of Peyer's patches, mesenteric lymph nodes, and postcapillary venules of gut lamina propria (LP).[8] Interaction of $\alpha4\beta7$ with MAdCAM-1 mediates the extravasation of naïve and activated leukocytes from blood to gut-associated lymphoid tissues and the LP. Increased MAdCAM-1 expression has been reported in active UC.[8,9] Recent studies that show induction of clinical remission in UC patients after immunoblockade of leukocyte trafficking support the importance of leukocyte homing in disease pathobiology.[10–12]

$\beta7$ integrin can also heterodimerize with αE integrin to mediate binding to E-cadherin expressed on epithelial cells. The $\alpha E\beta7$ integrin is expressed on subsets of T cells, dendritic cells, mast cells,[7] innate lymphoid cells,[13] and tumor-infiltrating NK cells.[14] Within the gut, the interaction between $\alpha E\beta7$ and E-cadherin enables retention of lymphocytes in the intraepithelial compartment. More than 90% of intraepithelial lymphocytes (IELs) and a minority of LP lymphocytes express $\alpha E\beta7$.[15] The proportion of mucosal T cells that express αE was higher in intestinal tissues compared with other organs, such as the lungs and spleen.[16] αE expression has been shown to enhance IEL activation,[17] promote antitumor cytotoxicity of T lymphocytes,[18,19] and modulate cell motility.[20]

The understanding of the role of $\alpha E\beta7$ integrin in both IEL and LP cells in the gut is evolving. In murine studies, IELs can act as effector memory T cells to protect the epithelium from pathogens.[21] There is emerging evidence that $\alpha E\beta7^+$ cells may play a pathogenic role in the gut, and aberrant activation of $\alpha E\beta7^+$ cells may contribute to inflammation and pathobiology of UC (unpublished data, 2014). $\alpha E\beta7^+$ memory $CD8^+$ T cells with the capacity to produce proinflammatory cytokines are highly enriched in the gut compared with other tissues.[16,22] αE^+CD4^+ and $CD8^+$ T cells from UC patients, but not control subjects, have an effector phenotype with increased expression of proinflammatory cytokines compared with controls (unpublished data, 2014). αE^+ cells from the gut also have high levels of perforin and granzyme A.[23] αE^+ intraepithelial type 1 innate lymphoid cells were also found to be increased in patients with Crohn's disease and contribute to the inflammatory process in anti-CD40–induced murine colitis.[13] Consistent with this, anti-αE treatment has been shown to attenuate experimental colitis in mice.[24]

Etrolizumab, a humanized monoclonal antibody against the $\beta7$ integrin subunit, blocks both $\alpha4\beta7$:MAdCAM-1 and $\alpha E\beta7$:E-cadherin interactions to reduce homing of leukocytes to the gut mucosa and retention of lymphocytes in the intraepithelial compartment, respectively. A recent phase 2 study of etrolizumab demonstrated efficacy relative to placebo in patients with moderate to severely active UC. Subsequent analyses of these data indicated that patients with high αE gene expression or αE^+ cell numbers in baseline colonic biopsies might have increased benefit.[11] In the current study, we evaluated baseline differences in colonic gene expression between patients who achieved clinical remission with etrolizumab in the phase 2 study compared with those who did not to identify additional predictive biomarkers of response. The relationship of these genes with etrolizumab therapeutic efficacy was then evaluated.

Materials and Methods

Patient Cohorts

Two independent cohorts of patients were included in this analysis: (1) UC patients enrolled in the phase 2 randomized double-blind placebo-controlled trial of etrolizumab[11] (referred to as cohort 1) and (2) UC patients and non-IBD controls concurrently enrolled in an observational study at a separate site not involved in the phase 2 study (referred to as cohort 2) (unpublished data, 2014). Predictive biomarkers of response to etrolizumab were identified in cohort 1, and gene expression in flow cytometry–sorted T cells was evaluated in cohort 2. In cohort 1, clinical remission was defined as total Mayo Clinic Score[25] ≤2, with no individual subscore >1, and mucosal healing was defined as endoscopic score ≤1.

Biopsy Collection

Colonic biopsies were collected from patients in cohort 1 during flexible sigmoidoscopy or full colonoscopy at screening, week 6, and week 10.[11] Biopsies were taken from the most inflamed area of the colon within 10 to 40 cm of the anal verge (avoiding necrotic areas) and placed into RNAlater (Life Technologies, Carlsbad, CA) or formalin.

In cohort 2, colonic biopsies were taken from inflamed and/or uninflamed areas of the colon and placed into RNAlater, formalin, or processed immediately for cell sorting.

RNA Isolation and Sequencing

RNAlater biopsies were homogenized using Tissuelyzer and RNA was isolated using the RNeasy Mini Kit (Qiagen, Hilden, Germany) according to manufacturer's instructions. RNA integrity was assessed using the Agilent RNA 6000 Pico Kit on Bioanalyzer (Agilent Technologies, Inc., Santa Clara, CA) and quantitated using the Invitrogen Quant-iT RNA Assay Kit (Life Technologies) or NanoDrop (Thermo Scientific, Waltham, MA).

Total RNA (RNA integrity number >5; 250 ng) was put into the Illumina TruSeq RNA Sample Preparation Kit v2 protocol and run in conjunction with Biomek liquid handling platforms (Beckman Coulter Life Sciences, Brea, CA). RNA libraries were evaluated using the Agilent 2200 TapeStation HighSensitivity D1K Tape and quantitative polymerase chain reaction (qPCR) with the KAPA Library Quantification Kit for Illumina sequencing. Then 2 nM of library (12 samples per lane) was loaded for cluster generation and sequenced on the Illumina HiSeq 2000 Sequencing System at 2×50 base pairs read length plus index read. Reads that passed quality filters were determined, and fastq files were generated by Illumina CASAVA v1.8.

Identification of Differentially Expressed Genes

Processing and analysis of the RNA sequencing data were performed using the R programming language (http://www.r-project.org) along with packages from the Bioconductor

project (http://bioconductor.org). Raw RNA sequencing reads were processed using the HTSeqGenie Bioconductor package. Reads were aligned to the reference human genome sequence (National Center for Biotechnology Information build 37) using the Genomic Short-Read Nucleotide Alignment Program algorithm.[26] Uniquely aligned read pairs that fell within exons were counted to estimate individual gene expression levels. For inclusion, genes were required to have >10 reads in ≥4 samples.

Two approaches were taken to identify differentially expressed genes in etrolizumab-treated patients: (1) identification of individual genes associated with clinical remission in response to etrolizumab and (2) gene-set enrichment using predefined groups of immune cell genes derived from comparisons of sorted immune cells defined by Abbas et al[27] (Supplementary Table 1).

To calculate differential expression, we used the DESeq2 Bioconductor package[28] that fits a negative binomial generalized linear model to determine the log-fold change and *P* value for differences between groups. The default library size estimation method was used to account for differences in sequencing depth. The response variable was clinical remission at the primary endpoint of the study.[11] Technical aspects of the sequencing runs and the endoscopic subscore at the screening visit were also incorporated in the model. Endoscopic subscore at screening was not prognostic of clinical remission at week 10 in cohort 1.[11] For our statistical analysis, nominal (nonmultiple test-corrected) *P* values were used to rank candidate genes associated with clinical remission.[11]

Gene set enrichment analysis was used to characterize differences between clinical remitters and nonremitters in anti-TNF−naïve patients treated with etrolizumab. This analysis was implemented using the GSEAlm Bioconductor package.[29] The Wald statistic generated by the DESeq2 algorithm was aggregated by summing the test statistics for a gene set and dividing by the square root of the gene-set size. This gene-set statistic was compared with a set of null statistics derived by permuting the clinical remission sample labels and recalculating the Wald statistic for differences between the permuted groups. An empirical *P* value was calculated by counting the number of permuted gene-set statistics that were more extreme (ie, further from 0) than the gene-set statistic calculated for the true sample labels.

Cell Sorting From Colonic Biopsies From Cohort 2

Colonic biopsies from cohort 2 were processed to a single-cell suspension. Mononuclear cells were extracted by incubation with 5 mM 1,4-dithiothreitol, followed by digestion with 1.5 mg/mL collagenase VIII and 0.05 mg/mL DNase I (Sigma, St Louis, MO for all reagents) then stained with Live/Dead stain (Life Technologies); CD45 PeCy5, TCR$\alpha\beta$ PeCy7, CD8α allophycocyanin Cy7, CD4 Pacific Blue, αE integrin fluorescein isothiocyanate, β7 integrin allophycocyanin (all from Biolegend, London, UK), and CD8β phycoerythrin (Beckman Coulter). TCR$\alpha\beta^{+}$CD4^{+} or TCR$\alpha\beta^{+}$CD8^{+} T cells were sorted based on their expression of αE and β7 integrin directly into RLT buffer (Qiagen) containing β-mercaptoethanol. RNA was isolated using PicoPure RNA isolation kit (Life Technologies). Purity of the sorted populations was assessed to ensure samples had ≥85% purity. Sorted T cells from inflamed biopsies were used for analysis in UC patients when available (11 of 13 patients).

Gene Expression Analysis by Quantitative Polymerase Chain Reaction

RNA isolated from RNAlater biopsies was reverse transcribed into complementary DNA using the High-Capacity cDNA Reverse Transcription Kit (Life Technologies). Gene expression levels were measured by qPCR using the BioMark HD System (Fluidigm, South San Francisco, CA) with TaqMan PreAmp Master Mix (Life Technologies) and reagents (Fluidigm, South San Francisco, CA) using Taqman Gene Expression assays of respective genes (Life Technologies), according to manufacturer's instructions. Target gene expression was normalized to glyceraldehyde-3-phosphate dehydrogenase (phosphorylating) expression using the ΔCt method. Biopsies with missing αE (n = 4) or *GZMA* (n = 1) due to study logistical issues and data quality control were not included.

The top 45 differentially expressed genes identified from RNA sequencing analyses were annotated to leukocyte subsets based on their mean expression level in flow cytometry sort-purified peripheral immune cells.[27] qPCR analysis of baseline colonic *GZMA* or αE expression was used to categorize patients into *GZMA*^{high} or αE^{high} (greater than or equal to median) and *GZMA*^{low} or αE^{low} (less than median) subgroups.

Immunohistochemistry Quantification

Formalin-fixed tissue samples were obtained from both cohort 1[11] and cohort 2 patients. Geboes scoring and immunohistochemistry of αE were performed according to the protocol described previously[11] and adapted for immunofluorescence for co-staining. For dual immunofluorescence studies in cohort 2, anti-granzyme A polyclonal goat IgG (R&D Systems, Minneapolis, MN) was incubated for 60 minutes at 37°C. Anti-goat Omnimap-HRP was used as detection, and 4′,6-diamidino-2-phenylindole and hematoxylin II were used to counterstain the sections (Ventana Medical Systems, Inc, Tucson, AZ).

Statistical Analysis

Statistical testing was performed using the Mann-Whitney test, Wilcoxon matched-pairs signed rank test, or the Fisher's exact test, as appropriate, using Prism (GraphPad Software Inc., La Jolla, CA) or JMP (SAS Institute Inc, Cary, NC). No adjustments for multiple comparisons were performed. Subgroup analyses using the sample median cutoff were performed for granzyme A and αE. Positive predictive value was defined as biomarker^{high} patients in remission/biomarker^{high} patients and negative predictive value as biomarker^{low} patients not in remission/biomarker^{low} patients.

Results

Patient Demographics and Baseline Characteristics

The demographics and baseline characteristics of patients who participated in cohort 1[11] (n = 110) and cohort 2 (n = 21; unpublished data, 2014) have been detailed.

Enrichment of T-Cell–Associated Genes in Baseline Biopsies of Anti–Tumor Necrosis Factor-Naïve Clinical Remitters Treated With Etrolizumab

In cohort 1 anti–TNF-naïve patients, T-cell–associated genes were significantly enriched at baseline in clinical remitters compared with nonremitters ($P < .05$; Figure 1*A*). Neutrophil-associated genes were significantly down-regulated in clinical remitters ($P < .01$; Figure 1*B*). Gene-set enrichment analysis of DC-, monocyte-, and B-cell–associated genes showed no significant baseline differences between clinical remitters and nonremitters (Supplementary Figure 1).

Clustering analysis of the top differentially expressed genes in anti–TNF-naïve etrolizumab-treated patients showed that the main cluster of clinical remitters had up-regulation of genes with higher expression in sort-purified T cells (*ITGAE*, *GZMA*, *GPR15*, *FGF9*, *PHF14*, *FAM125B*, *TMEM200A*, *TMIGD2*, *KLRB1*, *ECH1*, *FOXM1*, and *CPA2*) and down-regulation of genes with higher expression in sort-purified neutrophils (*VNN2*, *TMEM154*, and *LRRC4*; Supplementary Figure 2).

Increased Granzyme A (GZMA) in αE^+ T Cells From Ulcerative Colitis Patients

In flow cytometry–sorted T cells isolated from colonic biopsies from UC patients in cohort 2 (Supplementary Figure 3), *GZMA* gene expression was significantly up-regulated in $CD4^+\alpha E^+$ compared with $CD4^+\alpha E^-$ T cells ($P < .0001$; Figure 2*A*); the level of granzyme A in $CD4^+\alpha E^+$ cells was also significantly higher in UC patients compared with non-IBD controls ($P < .05$; Figure 2*A*). *GZMA* gene expression was positively correlated with αE gene expression in sorted $CD4^+\alpha E^+$ cells, but not $CD8^+\alpha E^+$ cells, from UC patients (Spearman $\rho = 0.76$; 95% confidence interval [CI]: 0.28–0.94; Figure 2*B*); other effector genes such as perforin and Fas ligand expression were also significantly positively correlated with *GZMA* and αE in sorted $CD4^+\alpha E^+$ cells (Supplementary Figure 4), but not $CD8^+\alpha E^+$ cells (data not shown), from UC patients. Consistent with data from cohort 2, gene expression of *GZMA* and *ITGAE* was positively correlated in baseline colonic biopsies from cohort 1 (etrolizumab: Spearman $\rho = 0.48$; 95% CI: 0.27–0.65; placebo: Spearman $\rho = 0.61$; 95% CI: 0.35–0.78; Figure 2*C*). Colonic biopsy *GZMA* expression was significantly correlated with the number of αE^+ cells in the crypt epithelium (epithelial-associated αE^+ cells) and LP in colonic biopsies from cohort 1 (crypt epithelium: Spearman $\rho = 0.45$; 95% CI: 0.21–0.64: LP: Spearman $\rho = 0.30$; 95% CI: 0.06–0.50; Figure 2*D*). Dual immunofluorescence analysis showed that granzyme A staining was limited to a subset of αE^+ cells in colonic tissue, with the majority of αE^+ granzyme A^+ cells appearing to localize to the crypt epithelium (Figure 2*E*). These data suggest that αE^+ cells may be a source of granzyme A in the colon.

Baseline Characteristics and Enrichment of Clinical Remission and Mucosal Healing Using ITGAE and GZMA

Both αE integrin (ITGAE) and granzyme A (GZMA) were identified by differential gene expression analysis. Enrichment of clinical remission (Figure 3*A*) and mucosal healing (Figure 3*B*) in response to etrolizumab was observed in cohort 1 patients with high baseline colonic biopsy *GZMA* gene expression (clinical remission: all patients (positive predictive value/negative predictive value): 100 mg, 41%/94%; 300 mg + LD, 18%/95%; anti–TNF-naïve (positive predictive value/negative predictive value): 100 mg,

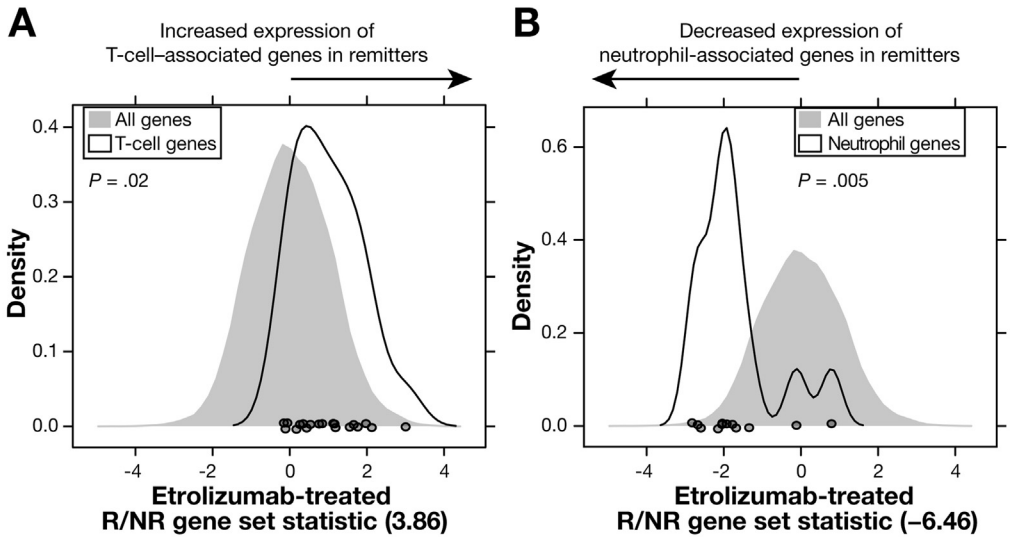

Figure 1. Differences in baseline colonic biopsy gene expression between clinical remitters and nonremitters treated with etrolizumab. Distribution of curated (*A*) T-cell– and (*B*) neutrophil-associated genes in baseline colonic biopsies of anti–TNF-naïve etrolizumab-treated patients. *P* value was empirically calculated by counting the number of permuted gene-set statistics that were more extreme than the gene-set statistic calculated for the true sample labels. X-axis represents clinical remitter to nonremitter gene-set statistic.

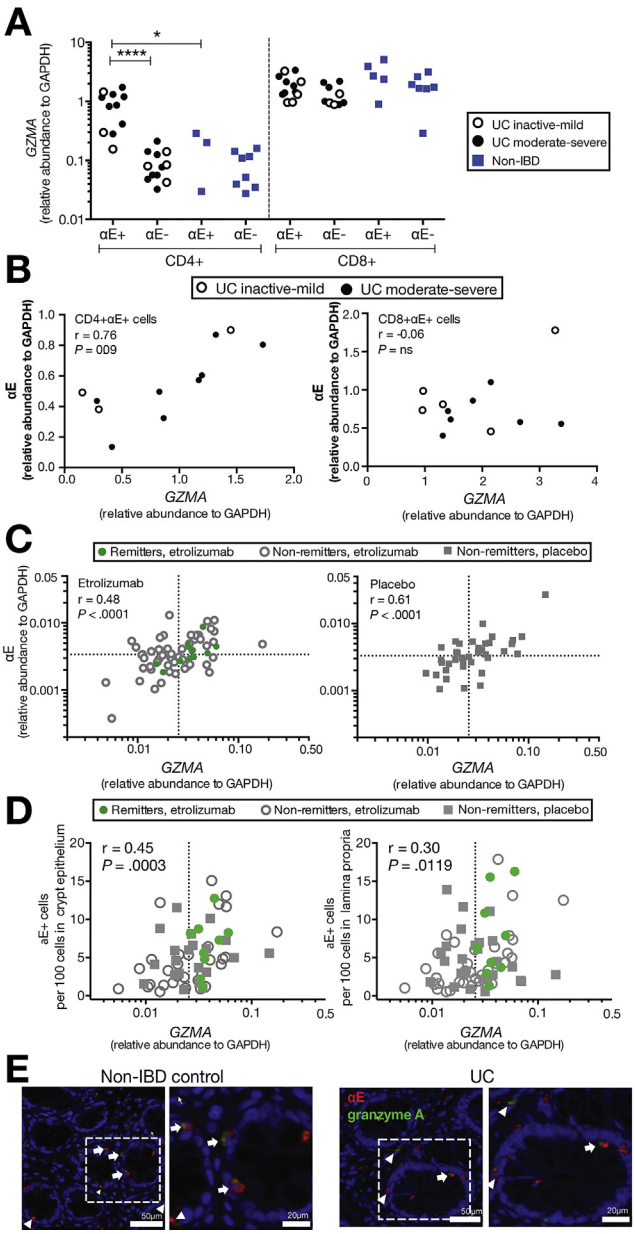

Figure 2. Increased granzyme A in αE^+ T cells in UC patients. (*A*) TCR$\alpha\beta^+$ $CD4^+$ and $CD8^+$ T cells from colonic biopsies from cohort 2 were sort purified by αE expression. $CD4^+\alpha E^+$ T cells from UC patients had increased granzyme A (*GZMA*) expression compared with sorted $CD4^+\alpha E^-$ T cells from UC patients and $CD4^+\alpha E^+$ T cells from non-IBD controls. (*B*) *GZMA* and αE gene expression was significantly correlated in sorted $CD4^+\alpha E^+$ T cells, but not sorted $CD8^+\alpha E^+$ T cells from UC patients in cohort 2. In cohort 1, *GZMA* gene expression was significantly correlated with (*C*) αE gene expression (*dotted lines* indicate qPCR median cutoff) and (*D*) the number of αE^+ cells in the epithelium and LP in colonic biopsies. (*E*) Representative immunofluorescence co-staining of granzyme A and αE in a colonic biopsy sample from cohort 2. *$P <$ .05; ****$P <$ .0001.

75%/88%; 300 mg + LD, 50%/100%). Enrichment of clinical remission in αE^{high} patients in cohort 1 has been detailed.[11] Enrichment of mucosal healing was observed in αE^{high} patients in cohort 1 in response to 100-mg etrolizumab (Supplementary Figure 5). The combination of *ITGAE* and *GZMA*, while resulting in small patient subsets, showed a further enrichment of clinical remission (Supplementary Table 2).

Baseline clinical characteristics were balanced across treatment groups in both the *ITGAE* and *GZMA* biomarker subgroups, with the exception of older age and lower immunosuppressant use in the $GZMA^{high}$ group compared with the $GZMA^{low}$ group (Supplementary Table 2). There was no significant difference in the distribution of baseline *GZMA* or αE[11] by previous anti-TNF use (Supplementary Figure 6). Although overall Mayo Clinic score was similar between αE subgroups, endoscopy score was slightly lower in the αE^{high} group (Supplementary Table 3). No difference was observed in the $GZMA^{high}$ and $GZMA^{low}$ subgroups for total Mayo Clinic score or subscores (Supplementary Table 3).

A subset of patients had biopsies available for histologic analysis.[11] αE^{low} patients had higher modified Geboes scores[30] at baseline than αE^{high} patients (mean ± SD, 2.3 ± 0.8 and 1.7 ± 0.9, respectively; $P <$ .01); no significant difference was observed between *GZMA* subgroups (Supplementary Table 2).

Post-Treatment Effects of Etrolizumab in Biomarker^{high} and Biomarker^{low} Patients

At baseline, the number of epithelial-associated αE^+ cells was significantly higher in both αE^{high} and $GZMA^{high}$ patients than αE^{low} and $GZMA^{low}$ patients, respectively (median ± median absolute deviation, 5.6 ± 2.6 in both αE^{high} and $GZMA^{high}$ vs 2.6 ± 1.6 and 2.9 ± 1.7 in αE^{low} and $GZMA^{low}$ patients respectively; $P <$ .01 both; Figure 4*A*). All epithelial-associated αE^+ cells were included in this analysis, as no co-stains (eg, CD3 or CD4) were used. Etrolizumab treatment significantly reduced the number of epithelial-associated αE^+ cells at week 10 in αE^{high} (median ± median absolute deviation, 33% ± 25%; $P <$ .05) and $GZMA^{high}$ patients (median ± median absolute deviation,: 36% ± 22%; $P <$ .01), while there was no significant reduction in epithelial-associated αE^+ cells in αE^{low} and $GZMA^{low}$ patients post-etrolizumab treatment (Figure 4*B*). Etrolizumab treatment also significantly changed gene expression in $GZMA^{high}$ etrolizumab-treated patients relative to placebo. T-cell–associated genes (αE, granzyme A, and granzyme B; $P <$ .05; Figure 5*A*) and cytokines and chemokines (interleukin 17F, interleukin 8, CCL4, and CXCL1; $P <$ .05; Figure 5*B*) were reduced in expression at week 10 in $GZMA^{high}$ etrolizumab-treated patients compared with placebo. There was no significant difference in these genes between placebo and etrolizumab-treated patients in the $GZMA^{low}$ subgroup at week 10. $GZMA^{high}$ patients had higher expression of αE, granzyme B, and CCL5 and lower expression of CXCL1 at baseline than $GZMA^{low}$ patients (Supplementary Figure 7*A*; $P <$ .05–$P <$ .001). Only CCL5 was significantly decreased at week 10 in αE^{high} etrolizumab-treated patients compared with placebo ($P <$ .05; Supplementary Figure 8); CCL5 was significantly higher in αE^{high} patients than αE^{low} patients at baseline ($P <$ .05; Supplementary Figure 7*B*).

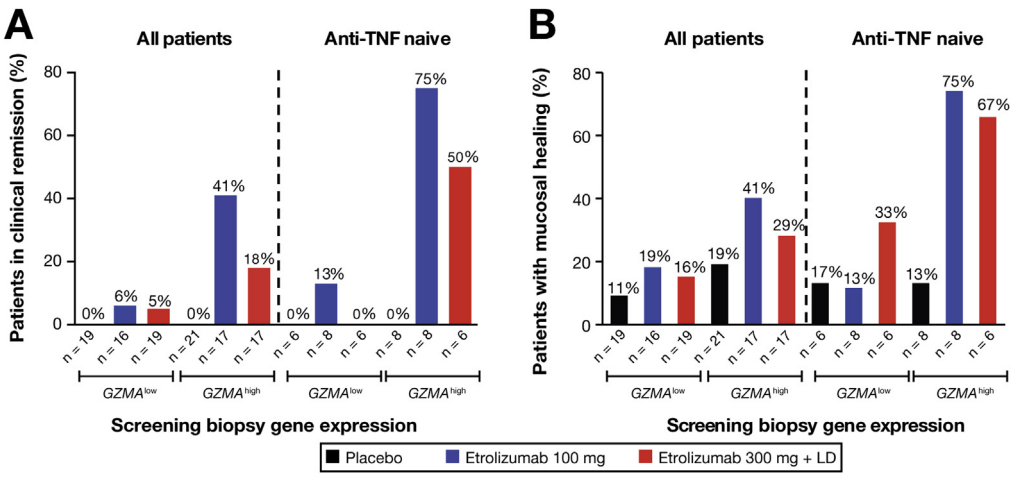

Figure 3. Clinical remission and mucosal healing by baseline *GZMA* expression. (*A*) Clinical remission and (*B*) mucosal healing by baseline *GZMA* gene expression. Baseline colonic biopsy qPCR median value was used to categorize patients as $GZMA^{high}$ (greater than or equal to median) or $GZMA^{low}$ (less than median). LD, loading dose; TNF, tumor necrosis factor.

Differences in histologic changes were observed at week 10 by biomarker subgroups. The modified Geboes score was significantly higher at baseline in αE^{low} patients and was significantly reduced at week 10 among etrolizumab-treated patients compared with those treated with placebo ($P < .01$; Supplementary Figure 9). The modified Geboes score was significantly decreased at week 10 in etrolizumab-treated $GZMA^{high}$ patients, but not $GZMA^{low}$ patients, compared with placebo ($P < .05$; Supplementary Figure 9). There were no apparent changes in the placebo arm in either biomarker subgroup.

Discussion

Drug therapies, such as etrolizumab, that selectively block leukocyte trafficking are emerging treatment options for UC.[12] Etrolizumab has demonstrated clinical efficacy in a phase 2 study of moderate to severely active UC, and a subset of patients with high colonic αE expression showed even greater benefits.[11] Identification of additional predictive biomarkers for response to treatment with etrolizumab could improve the efficiency of therapy for moderate to severely active UC through a personalized medicine approach. We evaluated gene expression post-hoc in baseline biopsies from anti−TNF-naïve UC patients treated with etrolizumab and found higher baseline expression of T-cell−associated genes, including αE integrin and granzyme A, in clinical remitters. αE gene expression was found to correlate with granzyme A gene expression, was significantly higher in $CD4^{+}\alpha E^{+}$ cells than $CD4^{+}\alpha E^{-}$ cells sorted from UC patients, and a subset of αE^{+} cells were found to co-express granzyme A in colonic tissue. Enrichment of clinical remission and mucosal healing was observed in both αE^{high},[11] and $GZMA^{high}$ patients. Some differences in baseline characteristics between biomarker subgroups were observed, including lower endoscopy and histologic scores in αE^{high} patients, but the clinical relevance is unclear. However, neither the endoscopy score nor histologic score at baseline were predictive of remission in response to etrolizumab at week 10 in cohort 1. Both αE^{high} and $GZMA^{high}$ patients had higher numbers of αE^{+} cells in crypt epithelium at baseline and showed decreased αE^{+} crypt-associated cells after etrolizumab treatment compared with placebo. In line with the previously reported reduction in gene expression in etrolizumab remitters,[11] we found a significant decrease in colonic biopsy gene expression of T-cell−associated genes and inflammatory cytokines and chemokines in $GZMA^{high}$ patients treated with etrolizumab relative to placebo. Both of these potential predictive biomarkers will be tested prospectively in phase 3 studies.

In this study, increased expression of T-cell−associated genes was found in baseline biopsies of anti−TNF-naïve patients who achieved clinical remission in response to etrolizumab. In contrast, no difference in immune cell types was observed in TNF-inadequate responder patients in comparison to anti−TNF-naïve patients using the same gene-set analysis in baseline biopsies (data not shown). Higher rates of efficacy were observed in this study in anti−TNF-naïve patients and the 100-mg dose group, which could be due to differential effects of etrolizumab on particular cell types or other reasons related to study powering or demographic differences, as discussed elsewhere.[11] The specificity and exclusivity of the gene lists have been discussed.[27] These cell-associated gene lists were generated based on relatively exclusive expression of genes in a particular cell type compared with other cell types.[27] Due to the small number of NK cell−specific genes and the fact that many of these genes were below the minimum expression threshold used in the analysis, our findings on NK gene-set enrichment were inconclusive (data not shown). Minor cell populations not included in sorted gene sets,[27] such as innate lymphoid cells and NKT cells, may also express some of the genes identified as exclusively expressed.

Higher baseline levels of 2 biomarkers found predominantly on T cells, αE integrin and granzyme A, enriched for clinical remission after etrolizumab treatment. Granzyme A co-localized with αE expression in colonic biopsies, suggesting that αE^{+} cells could be a key source of granzyme A in the colon. Granzyme A, a serine protease present in activated and cytotoxic NK, NKT, and T cells,[31] lacks direct cytotoxic activity at low concentrations, but has been implicated in the release of inflammatory cytokines, such as interleukin 1β and TNFα.[32] Granzyme A has been shown to

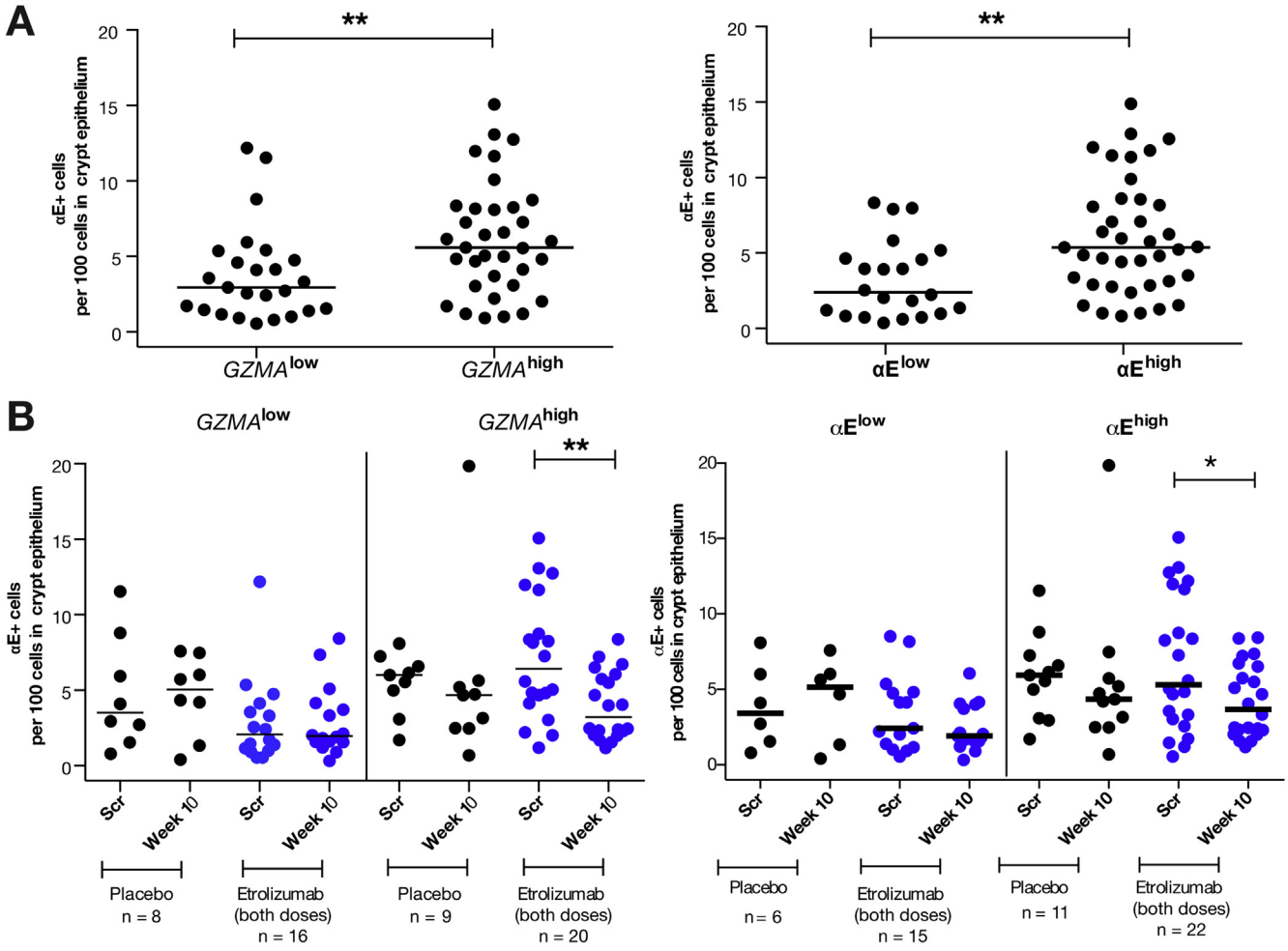

Figure 4. Effect of etrolizumab on epithelial crypt-associated αE^+ cells by biomarker stratification. Epithelial crypt-associated αE^+ cells were counted before and after treatment with etrolizumab or placebo in cohort 1. (*A*) Baseline distribution of epithelial crypt-associated αE^+ cells in *GZMA*^{high} or αE^{high} (greater than or equal to median) or *GZMA*^{low} or αE^{low} (less than median) patients where baseline colonic biopsy qPCR median value was used to categorize patients. (*B*) Change in epithelial crypt-associated $\alpha E+$ cells in *GZMA*^{high} or αE^{high} and *GZMA*^{low} or αE^{low} patients after treatment with etrolizumab (combined dose groups) or placebo. *$P < .05$; **$P < .01$. Scr, screening.

induce cleavage of extracellular matrix components, such as fibronectin and proteoglycan,[33] to potentially facilitate cell migration. Emergence of granzyme A−expressing human immunodeficiency virus−specific T cells has been associated with slower human immunodeficiency virus disease progression.[34] Although further studies will be required to evaluate the role of αE^+ granzyme A^+ cells in intestinal mucosa, the known functions are consistent with those of an effector cell phenotype.

Differences in baseline biopsy gene expression were observed based on biomarker status. Heterogeneity was observed in baseline measurements and individual patient data were shown to highlight variability where possible. Small numbers of samples in placebo groups should also be noted. Baseline *CCL5* was significantly higher in the αE^{high} subgroup than the αE^{low} subgroup, indicating that the αE^{high} environment may be associated with increased T-cell infiltration. *GZMA*^{high} patients had significantly increased *CCL5*, but decreased *CXCL1*, at baseline than *GZMA*^{low} patients. CCL5 is a chemoattractant for peripheral memory T-helper cells, while CXCL1 is a chemoattractant for neutrophils. *GZMA*^{high} patients may have increased recruitment of activated T cells and altered neutrophil infiltration. These findings support the benefits of using both of these biomarkers for the identification of UC patients likely to respond to etrolizumab therapy. Although $\alpha E\ \beta 7^+$ cells also expressed $\alpha 4$,[10] post-hoc analysis suggests that $\alpha 4$ is a pharmacodynamic[10] but not a predictive biomarker of etrolizumab (data not shown). The value of αE and *GZMA* as predictive biomarkers could be due to their specificity as surrogate markers of a subset of effector T cells that are impacted by etrolizumab.

Changes in gene expression post treatment were also different based on biomarker status, with significant effects observed when substratifying patients based on *GZMA* expression, supporting the idea that *GZMA* may be a promising biomarker for etrolizumab response. Granzyme A marks a subpopulation of αE^+ T cells in gut mucosa, and we

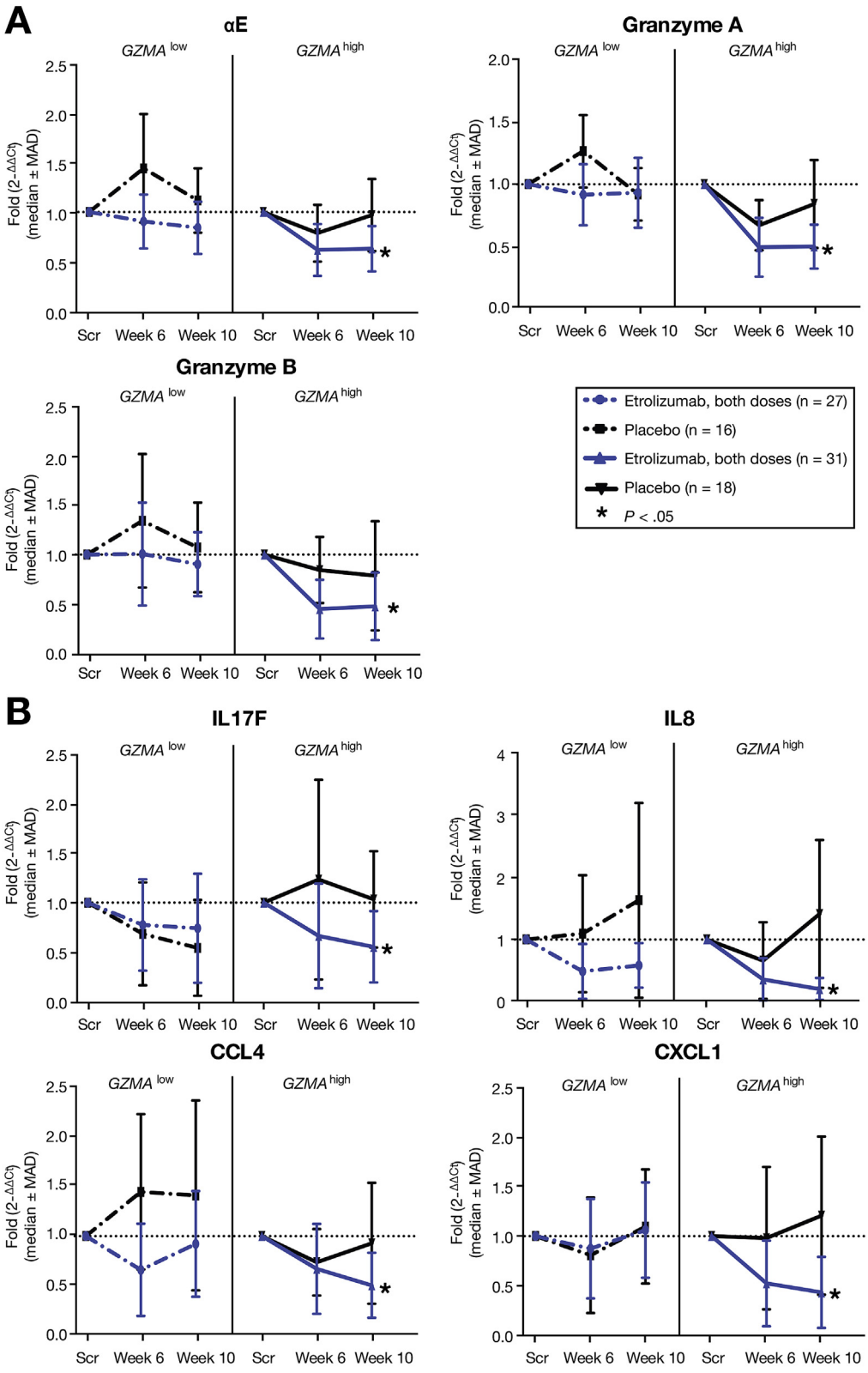

Figure 5. Effect of etrolizumab on colonic tissue gene expression by granzyme A stratification. Colonic biopsy gene expression was assessed by qPCR before and after treatment with etrolizumab (combined dose groups) or placebo in cohort 1. (*A*) T-cell–associated genes and (*B*) cytokines and chemokines were reduced in colonic tissue after treatment with etrolizumab in *GZMA*^{high} (greater than or equal to median) but not *GZMA*^{low} (less than median) patients relative to placebo. Data are presented as fold ($2^{-\Delta\Delta Ct}$) group median ± median absolute deviation. *P < .05 vs placebo. Scr, screening.

observed a positive correlation between *GZMA* and αE gene expression in colonic biopsies as well as in sorted CD4$^+$αE$^+$ cells. In sorted CD4$^+$αE$^+$ cells, the expression of *GZMA* was significantly up-regulated in UC patients relative to controls. These biomarkers were also positively correlated with effector molecules, such as Fas ligand and perforin, suggesting that these CD4$^+$ cells might have acquired effector phenotypes of cytolytic lymphocytes (CD4$^+$ cytotoxic T

lymphocytes). $CD4^+$ cytotoxic T lymphocytes were reported to be associated with chronic immune activation, such as in chronic viral infections[35–37] and in inflammatory disease, including CD[38] and rheumatoid arthritis.[39] Recent work supports that this cell population may also play a role in UC, where higher expression of inflammatory cytokines are observed in $CD4^+\alpha E^+$ T cells in inflamed biopsies from UC patients compared with non-IBD controls (unpublished data, 2014). The enhanced benefits of etrolizumab on clinical remission and mucosal healing in patients with high *GZMA* and αE gene expression in baseline colonic biopsies support the hypothesis that increased activation and retention of T cells in the gut may play a crucial role in the pathobiology of UC. It should be noted that the sample size in these studies is small and further analysis will be required to test this hypothesis. In addition, the specificity of these observations for etrolizumab therapy in comparison with other therapies will need to be evaluated.

We observed a greater histologic improvement from baseline in etrolizumab-treated αE^{low} patients, suggesting increased benefits in microscopic healing in these patients than αE^{high} patients. Enrichment of clinical benefit was observed in αE^{high} patients, but the lower histologic grade at baseline in αE^{high} patients might have led to less sensitivity for histologic changes after treatment. Histologic improvement did not translate to clinical benefits in αE^{low} patients within the 10-week trial period of cohort 1, but patients did achieve a histologic score similar to baseline levels of αE^{high} patients by the end of the study, and a longer treatment period may be needed to assess the clinical benefits after histologic healing. Compared with αE subgroups, *GZMA* subgroups had balanced histologic and endoscopic scores at baseline, but enriched clinical remission was only observed in $GZMA^{high}$ patients.

Immunohistochemistry assessment of granzyme A expression in a subset of αE^+ cells may be equally important for patient identification. Epithelial erosion or loss of intestinal epithelial cells that express E-cadherin in the setting of active UC could further reduce the anchoring of αE^+ cells in the epithelium and therefore the quantification of αE transcripts by qPCR. Geboes erosion subscore, but not crypt destruction or the presence of neutrophils in the epithelium (data not shown), was higher in αE^{low} patients than αE^{high} patients at baseline, suggesting that αE^{low} patients may have increased inflammation involving erosion of the epithelium without other differences in active disease measured by histology. However, histologic scores were not different between $GZMA^{high}$ and $GZMA^{low}$ patients. The absence of baseline differences between *GZMA* subgroups suggests that granzyme A^+ cells may be less affected by epithelial loss and therefore be a more robust and stable biomarker without the confounding effects of epithelial erosions that may impact αE levels.

The potential predictive biomarker profile identified in this study is the first of its kind in a moderate to severely active UC patient population and could pave the way for a personalized medicine approach to therapeutic decision making. The pathobiology of IBD is complex, and customizing therapy to a patient's predictive biomarker profile will be important in creating optimal therapeutic responses and tailoring therapy for patients. Larger studies are underway to validate the findings of this study, with prospective analyses of baseline biomarker levels and exploration of clinically relevant biomarker cutoffs to test for enriched response to etrolizumab.

Supplementary Material

Note: To access the supplementary material accompanying this article, visit the online version of *Gastroenterology* at www.gastrojournal.org, and at http://dx.doi.org/10.1053/j.gastro.2015.10.041.

References

1. Ordas I, Eckmann L, Talamini M, et al. Ulcerative colitis. Lancet 2012;380:1606–1619.
2. Bach SP, Mortensen NJ. Ileal pouch surgery for ulcerative colitis. World J Gastroenterol 2007;13:3288–3300.
3. Ananthakrishnan AN. Personalizing therapy for inflammatory bowel diseases. Expert Rev Gastroenterol Hepatol 2013;7:549–558.
4. Loftus EV Jr, Davis KL, Wang CC, et al. Treatment patterns, complications, and disease relapse in a real-world population of patients with moderate-to-severe ulcerative colitis initiating immunomodulator therapy. Inflamm Bowel Dis 2014;20:1361–1367.
5. Kobayashi K, Asakura H, Hamada Y, et al. T lymphocyte subpopulations and immunoglobulin-containing cells in the colonic mucosa of ulcerative colitis; a morphometric and immunohistochemical study. J Clin Lab Immunol 1988;25:63–68.
6. Neurath MF, Weigmann B, Finotto S, et al. The transcription factor T-bet regulates mucosal T cell activation in experimental colitis and Crohn's disease. J Exp Med 2002;195:1129–1143.
7. Gorfu G, Rivera-Nieves J, Ley K. Role of beta7 integrins in intestinal lymphocyte homing and retention. Curr Mol Med 2009;9:836–850.
8. Briskin M, Winsor-Hines D, Shyjan A, et al. Human mucosal addressin cell adhesion molecule-1 is preferentially expressed in intestinal tract and associated lymphoid tissue. Am J Pathol 1997;151:97–110.
9. Arihiro S, Ohtani H, Suzuki M, et al. Differential expression of mucosal addressin cell adhesion molecule-1 (MAdCAM-1) in ulcerative colitis and Crohn's disease. Pathol Int 2002;52:367–374.
10. Feagan BG, Rutgeerts P, Sands BE, et al. Vedolizumab as induction and maintenance therapy for ulcerative colitis. N Engl J Med 2013;369:699–710.
11. Vermeire S, O'Byrne S, Keir M, et al. Etrolizumab as induction therapy for ulcerative colitis: a randomised, controlled, phase 2 trial. Lancet 2014;384(9940):309–318.
12. Thomas S, Baumgart DC. Targeting leukocyte migration and adhesion in Crohn's disease and ulcerative colitis. Inflammopharmacology 2012;20:1–18.
13. Fuchs A, Vermi W, Lee JS, et al. Intraepithelial type 1 innate lymphoid cells are a unique subset of IL-12- and

IL-15-responsive IFN-gamma-producing cells. Immunity 2013;38:769–781.
14. Webb JR, Milne K, Watson P, et al. Tumor-infiltrating lymphocytes expressing the tissue resident memory marker CD103 are associated with increased survival in high-grade serous ovarian cancer. Clin Cancer Res 2014; 20:434–444.
15. Cepek KL, Parker CM, Madara JL, et al. Integrin alpha E beta 7 mediates adhesion of T lymphocytes to epithelial cells. J Immunol 1993;150:3459–3470.
16. Sathaliyawala T, Kubota M, Yudanin N, et al. Distribution and compartmentalization of human circulating and tissue-resident memory T cell subsets. Immunity 2013; 38:187–197.
17. Monk T, Spencer J, Cerf-Bensussan N, et al. Stimulation of mucosal T cells in situ with anti-CD3 antibody: location of the activated T cells and their distribution within the mucosal micro-environment. Clin Exp Immunol 1988; 74:216–222.
18. Le Floc'h A, Jalil A, Vergnon I, et al. Alpha E beta 7 integrin interaction with E-cadherin promotes antitumor CTL activity by triggering lytic granule polarization and exocytosis. J Exp Med 2007;204:559–570.
19. Djenidi F, Adam J, Goubar A, et al. CD8+CD103+ Tumor-infiltrating lymphocytes are tumor-specific tissue-resident memory T cells and a prognostic factor for survival in lung cancer patients. J Immunol 2015; 194:3475–3486.
20. Schlickum S, Sennefelder H, Friedrich M, et al. Integrin alpha E(CD103)beta 7 influences cellular shape and motility in a ligand-dependent fashion. Blood 2008;112:619–625.
21. Masopust D, Vezys V, Wherry EJ, et al. Cutting edge: gut microenvironment promotes differentiation of a unique memory CD8 T cell population. J Immunol 2006; 176:2079–2083.
22. Sheridan BS, Lefrancois L. Regional and mucosal memory T cells. Nat Immunol 2011;12:485–491.
23. Annunziato F, Cosmi L, Liotta F, et al. CXCR3 and alphaEbeta7 integrin identify a subset of CD8+ mature thymocytes that share phenotypic and functional properties with CD8+ gut intraepithelial lymphocytes. Gut 2006;55:961–968.
24. Ludviksson BR, Strober W, Nishikomori R, et al. Administration of mAb against alpha E beta 7 prevents and ameliorates immunization-induced colitis in IL-2-/- mice. J Immunol 1999;162:4975–4982.
25. Schroeder KW, Tremaine WJ, Ilstrup DM. Coated oral 5-aminosalicylic acid therapy for mildly to moderately active ulcerative colitis. A randomized study. N Engl J Med 1987;317:1625–1629.
26. Wu TD, Nacu S. Fast and SNP-tolerant detection of complex variants and splicing in short reads. Bioinformatics 2010;26:873–881.
27. Abbas AR, Baldwin D, Ma Y, et al. Immune response in silico (IRIS): immune-specific genes identified from a compendium of microarray expression data. Genes Immun 2005;6:319–331.
28. Love MI, Huber W, Anders S. Moderated estimation of fold change and dispersion for RNA-seq data with DESeq2. Genome Biol 2014;15:550.
29. Jiang Z, Gentleman R. Extensions to gene set enrichment. Bioinformatics 2007;23:306–313.
30. Lemmens B, Arijs I, Van Assche G, et al. Correlation between the endoscopic and histologic score in assessing the activity of ulcerative colitis. Inflamm Bowel Dis 2013;19:1194–1201.
31. Grossman WJ, Verbsky JW, Tollefsen BL, et al. Differential expression of granzymes A and B in human cytotoxic lymphocyte subsets and T regulatory cells. Blood 2004;104:2840–2848.
32. Joeckel LT, Bird PI. Are all granzymes cytotoxic in vivo? Biol Chem 2014;395:181–202.
33. Anthony D, Andrews D, Watt S, et al. Functional dissection of the granzyme family: cell death and inflammation. Immunol Rev 2010;235:73–92.
34. Soghoian DZ, Jessen H, Flanders M, et al. HIV-specific cytolytic CD4 T cell responses during acute HIV infection predict disease outcome. Sci Transl Med 2012; 4:123ra25.
35. Appay V, Zaunders JJ, Papagno L, et al. Characterization of CD4(+) CTLs ex vivo. J Immunol 2002; 168:5954–5958.
36. Casazza JP, Betts MR, Price DA, et al. Acquisition of direct antiviral effector functions by CMV-specific CD4+ T lymphocytes with cellular maturation. J Exp Med 2006; 203:2865–2877.
37. Haigh TA, Lin X, Jia H, et al. EBV latent membrane proteins (LMPs) 1 and 2 as immunotherapeutic targets: LMP-specific CD4+ cytotoxic T cell recognition of EBV-transformed B cell lines. J Immunol 2008;180:1643–1654.
38. **Allez M, Tieng V**, Nakazawa A, et al. CD4+NKG2D+ T cells in Crohn's disease mediate inflammatory and cytotoxic responses through MICA interactions. Gastroenterology 2007;132:2346–2358.
39. Pawlik A, Ostanek L, Brzosko I, et al. The expansion of CD4+CD28- T cells in patients with rheumatoid arthritis. Arthritis Res Ther 2003;5:R210–R213.

Author names in bold designate shared co-first authorship.

Received June 22, 2015. Accepted October 22, 2015.

Reprint requests
Address requests for reprints to: Mary E. Keir, PhD, Genentech Inc, 1 DNA Way, South San Francisco, California. e-mail: keir.mary@gene.com; fax: (650) 742-4863.

Acknowledgments
The authors are grateful to the patients and investigators who participated in the etrolizumab phase 2 study. This study was sponsored by Genentech, Inc, a member of the Roche group. The authors thank David Choy, Franklin Fuh, and Carrie Looney for data analyses and Marna Williams and Teresa Ramirez Montagut for scientific input.

Jackson G. Egan's current affiliation is Amgen, South San Francisco, California.

Conflicts of interest
The authors disclose the following: Gaik W. Tew, Jason A. Hackney, Diana Luca, Lauri Diehl, Jeff Eastham Anderson, Sharon O'Byrne, and Mary E. Keir are employees of Genentech Inc. Jackson G. Egen is an employee of Amgen, Inc and a former employee of Genentech Inc. Deena Gibbons has served on advisory committees or review panels for Genentech Inc. and Cerimon Pharmaceuticals. Christopher A. Lamb has received research/grant support and/or nonfinancial support from Genentech, Wellcome Trust, Techlab, Immundiagnostik, Roche Tissue Diagnostics, Shire Pharmaceuticals UK, Falk Foundation, and Merck Sharp & Dohme. Severine Vermeire has received research/grant support from UCB, has received speaker fees from Abbott

Laboratories/AbbVie, Ferring Pharmaceuticals, MSD, Merck/Schering-Plough, and UCB, has served on advisory committees or review panels for Ferring Pharmaceuticals, Pfizer, MSD, and Shire, and has done consulting for AstraZeneca Pharmaceuticals and Ferring Pharmaceuticals (employment, spouse). John C. Mansfield has served on advisory committees or review panels for Abbott Laboratories/AbbVie and Genentech, and has received speaker fees from Ferring Pharmaceuticals, grants from Wellcome Trust and Genentech, nonfinancial support from Genentech, Roche Tissue Diagnostics, Techlab, and Immundiagnostik, personal fees from Genentech, Takeda, Sanofi, and Tillots; and other from Tillotts and Abbott. Brian G. Feagan has received research/grant support from Genentech, GlaxoSmithKline, has done consulting for Abbott Laboratories/AbbVie, Actogenix, Albireo, Amgen, AstraZeneca, Avaxia Biologics, Axcan, Baxter, Boehringer Ingelheim, Bristol-Myers Squibb, Calypso Biotech, Celgene, Elan/Biogen Idec, enGene, Ferring Pharmaceuticals, Roche/Genentech, gIcare pharma, Gilead, Given Imaging, GlaxoSmithKline, Ironwood Pharmaceuticals, Janssen Biotech, Johnson & Johnson/Janssen Pharmaceuticals, Kyowa Kakko Kirin, Lexicon Pharmaceuticals, Eli Lilly and Company, Merck, Millennium, Nektar, Novo Nordisk A/S, Pfizer, Pfizer/Wyeth, Prometheus Therapeutics and Diagnostics, Receptos, Salix Pharmaceuticals, Serono, Shire, Sigmoid Pharma, Synergy Pharmaceuticals, Takeda Pharmaceutical Company, Teva Pharmaceutical Industries, Tillotts Pharma AG, UCB, Warner Chilcott, Zealand Pharma, and Zyngenia, has received speakers fees from Abbott Laboratories/AbbVie, Johnson & Johnson/Janssen Pharmaceuticals, Warner Chilcott, and UCB, and has served on advisory committees or review panels for Abbott Laboratories/AbbVie, Amgen, AstraZeneca, Avaxia Biologics, Bristol-Myers Squibb, Celgene Biotech, and Novartis Pharma AG. Gert A. Van Assche has received research/grant support from Abbott Laboratories/A, Janssen Biotech, Elan/Biogen Idec, Ferring Pharmaceuticals, Johnson & Johnson/Janssen Pharmaceuticals, Merck, Novartis, Novo Nordisk A/S, Pfizer, Prometheus Laboratories, Salix Pharmaceuticals, Takeda Pharmaceutical Company, Teva Pharmaceutical Industries, Tillotts Pharma AG, and UCB. Julian Panes has received research/grant support from Abbott Laboratories/AbbVie, and MSD, has served on advisory committees or review panels for Abbott Laboratories/AbbVie, Bristol-Myers Squibb, Genentech, MSD, Pfizer, Roche, TopiVert, and TiGenix/Cellerix, and received personal fees from Boehringer-Ingelheim and Nutrition Science Partners. Daniel C. Baumgart has received research/grant support from Abbott Laboratories/AbbVie, Hitachi, and Shire, has done consulting for Abbott Laboratories/AbbVie, Celgene, Genentech, MSD, Pfizer, and has received speaker fees from Abbott Laboratories/AbbVie, the Falk Foundation, Ferring Pharmaceuticals, MSD, Shire, and TiGenix/Cellerix. Stefan Schreiber has served on advisory committees or review panels for Abbott Laboratories/AbbVie, Genentech, MSD, Pfizer, and Takeda Pharmaceutical Company, and has received speaker fees from Abbott Laboratories/AbbVie, MSD, and Takeda Pharmaceutical Company. Iris Dotan has served on advisory committees or review panels for Genentech, Janssen Biotech, Pfizer, and Atlantic Healthcare, has done consulting for BioLineRx, and has received speaker fees from Abbott Laboratories/Abbvie, the Falk Foundation, Ferring Pharmaceuticals, and Janssen Biotech. William J. Sandborn has received research/grant support from Bristol-Myers Squibb, Genentech, GlaxoSmithKline, Janssen Biotech, Novartis, Pfizer, Procter & Gamble Pharmaceuticals, Shire, Takeda Oncology Company/Millennium Pharmaceuticals, and UCB, has received speaker fees from Bristol-Myers Squibb and Janssen Biotech, has done consulting for ActoGeniX NV, AGI Therapeutics, ALBA Therapeutics, Albireo, Alfa Wassermann, Amgen, AM-Pharma, Anaphore, Astellas Pharma, Athersys, Atlantic Healthcare, Aptalis Pharma, Bio Balance, Boehringer Ingelheim, Bristol-Myers Squibb, Celgene, Celek Pharmaceuticals, Cerimon Pharmaceuticals, ChemoCentryx, CoMentis, Cosmo Pharmaceuticals, Coronado Biosciences, Cytokine Pharmasciences, Eagle Pharmaceuticals, Eisai, Elan, Eli Lilly and Company, enGene, Enteromedics, Exagen Diagnostics, Ferring Pharmaceuticals, Flexion Therapeutics, Funxional Therapeutics, Genentech, Genzyme, Gilead, Given Imaging, GlaxoSmithKline, GlaxoSmithKline/Sirtris Pharmaceuticals, Human Genome Sciences, Ironwood Pharmaceuticals, Janssen Biotech, KaloBios, Lexicon Pharmaceuticals, Lycera, Meda Pharmaceuticals, Merck, Merck Serono, KYORIN Pharmaceuticals, Novo Nordisk A/S, NPS Pharmaceuticals, Optimer Pharmaceuticals, Orexigen Therapeutics, PDL BioPharma, Pfizer, Pfizer/Wyeth, Procter & Gamble, Prometheus Laboratories, ProtAb, PurGenesis Technologies, Receptos, Relypsa, Salient Pharmaceuticals, Salix Pharmaceuticals, Santarus, Merck/Schering-Plough, Shire, Sigmoid Pharma, SLA Pharma AG, Takeda Oncology Company/Millennium Pharmaceuticals, Targacept, Teva Pharmaceutical Industries, Therakos, TiGenix/Cellerix, Tillotts Pharma AG, UCB, Viamet Pharmaceuticals, VBL Therapeutics, and Warner Chilcott. John A. Kirby has received research/grant support from Genentech and GlaxoSmithKline. Peter M. Irving has received grant/research support form AbbVie, MSD, has served on advisory committees or review panels for AbbVie, MSD, Vifor, Genentech Inc., Takeda, Warner Chilcott, Falk and Pharmacosmos and has received speaker fees for AbbVie, MSD, Ferring, Warner Chilcott, Shire and Johnson and Johnson. Gert De Hertogh has done consulting for Shire, Galapagos NV, Genentech, Janssen AbbVie, Merck, and University of Leuven, has done consulting for Abbott Laboratories/Abbvie, Bristol-Myers Squibb, Johnson & Johnson/Janssen Pharmaceuticals, Merck, Robarts Imaging, Takeda Pharmaceutical Company, and UCB, and has received speaker fees from Abbott Laboratories/AbbVie, Aptalis, Ferring Pharmaceuticals, and Merck. Paul Rutgeerts has received research/grant support from Abbott Laboratories/AbbVie, Janssen Biotech, Merck, UCB, has done consulting for Abbott Laboratories/AbbVie, Actogenix, Amgen, Bristol-Myers Squibb, Dr Falk Pharmaceuticals, Genentech, Janssen Biotech, Merck, Neovacs, Pfizer, Robarts Imaging, Takeda Oncology Company/Millennium Pharmaceuticals, Tillotts Pharma AG, and UCB, and has received speaker fees from Abbott Laboratories and Merck. Adrian Hayday has received compensation for consulting from HS-Lifesciences and ImmunoQure, has received grant/research support from ImmunoQure and Genentech Inc., has served on advisory committees or review panels for HS-Lifesciences and ImmunoQure, and has received compensation for speaking and teaching from MedImmune.

Funding

Christopher Lamb was supported by a grant from the Wellcome Trust (093885/Z/10/Z).

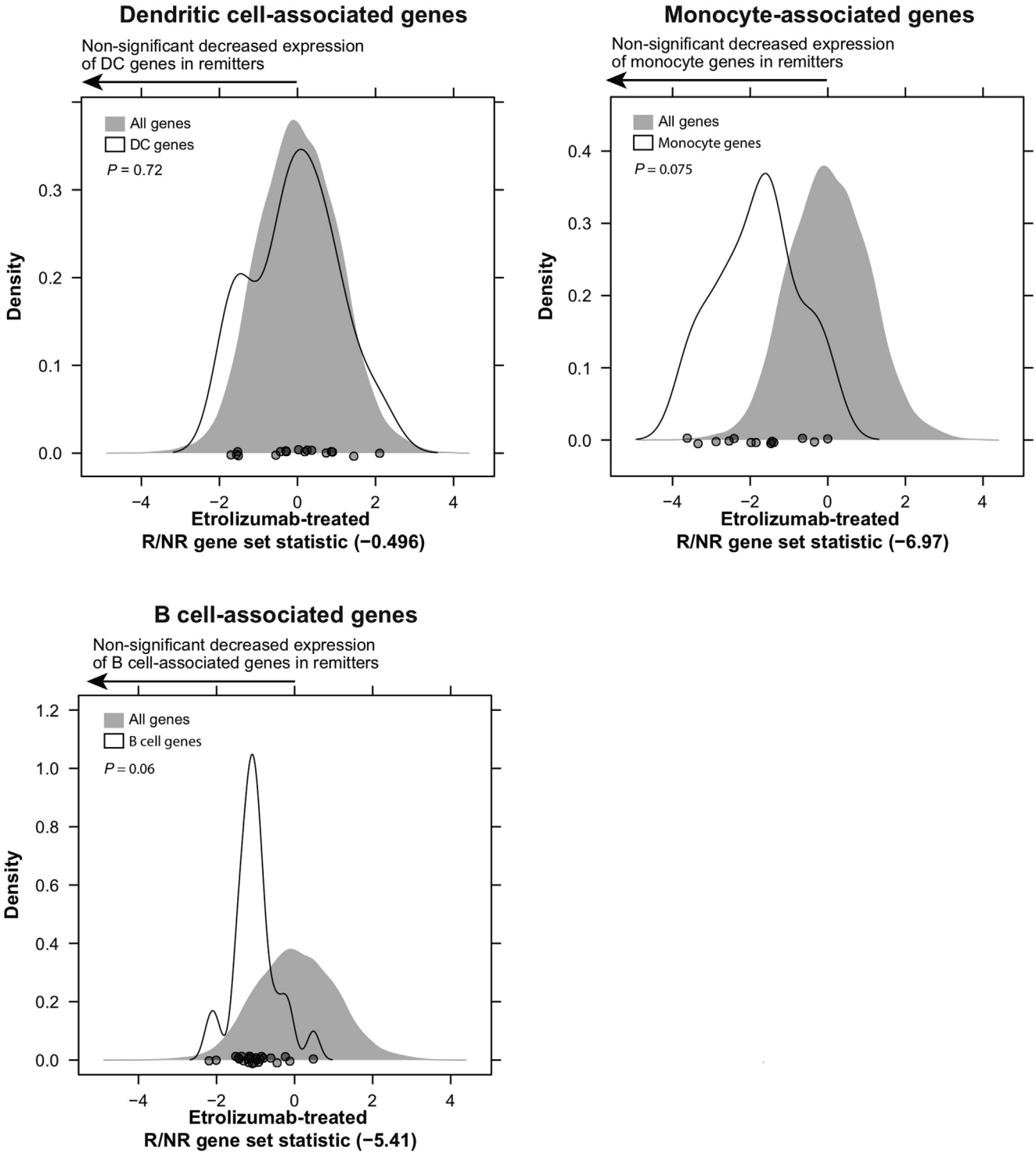

Supplementary Figure 1. Differences in baseline colonic biopsy gene expression between anti−TNF-naïve etrolizumab-treated clinical remitters and nonremitters. Distribution of curated DC-, monocyte-, and B-cell−associated genes in baseline colonic biopsies of anti−TNF-naïve etrolizumab-treated patients. *P* value is empirically calculated by counting the number of permuted gene-set statistics that were more extreme than the gene-set statistic calculated for the true sample labels. X-axis represents clinical remitter to nonremitter gene-set statistic.

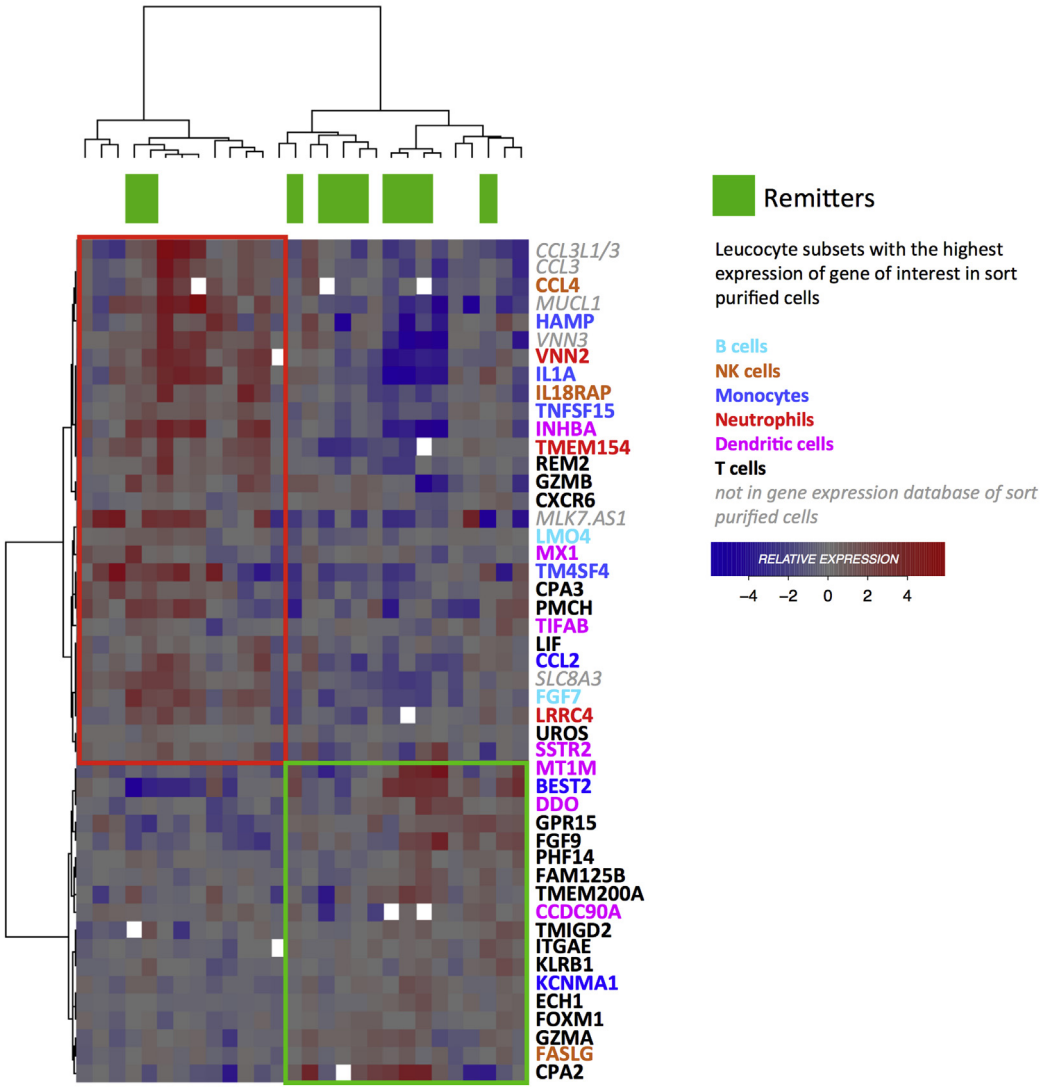

Supplementary Figure 2. Top differentially expressed genes between anti-TNF–naïve etrolizumab-treated clinical remitters and nonremitters at baseline. Dendrogram showing unsupervised clustering analysis of top differentially expressed genes between anti-TNF–naïve etrolizumab-treated clinical remitters and nonremitters, as measured by qPCR in baseline colonic biopsies from all etrolizumab-treated patients in cohort 1. Each gene is color coded to reflect the leukocyte subsets with the highest expression of the gene of interest based on gene expression database of flow cytometry sort-purified cells.[27] Genes shown in *gray* are not listed in the database or have low expression across all leukocyte subsets.

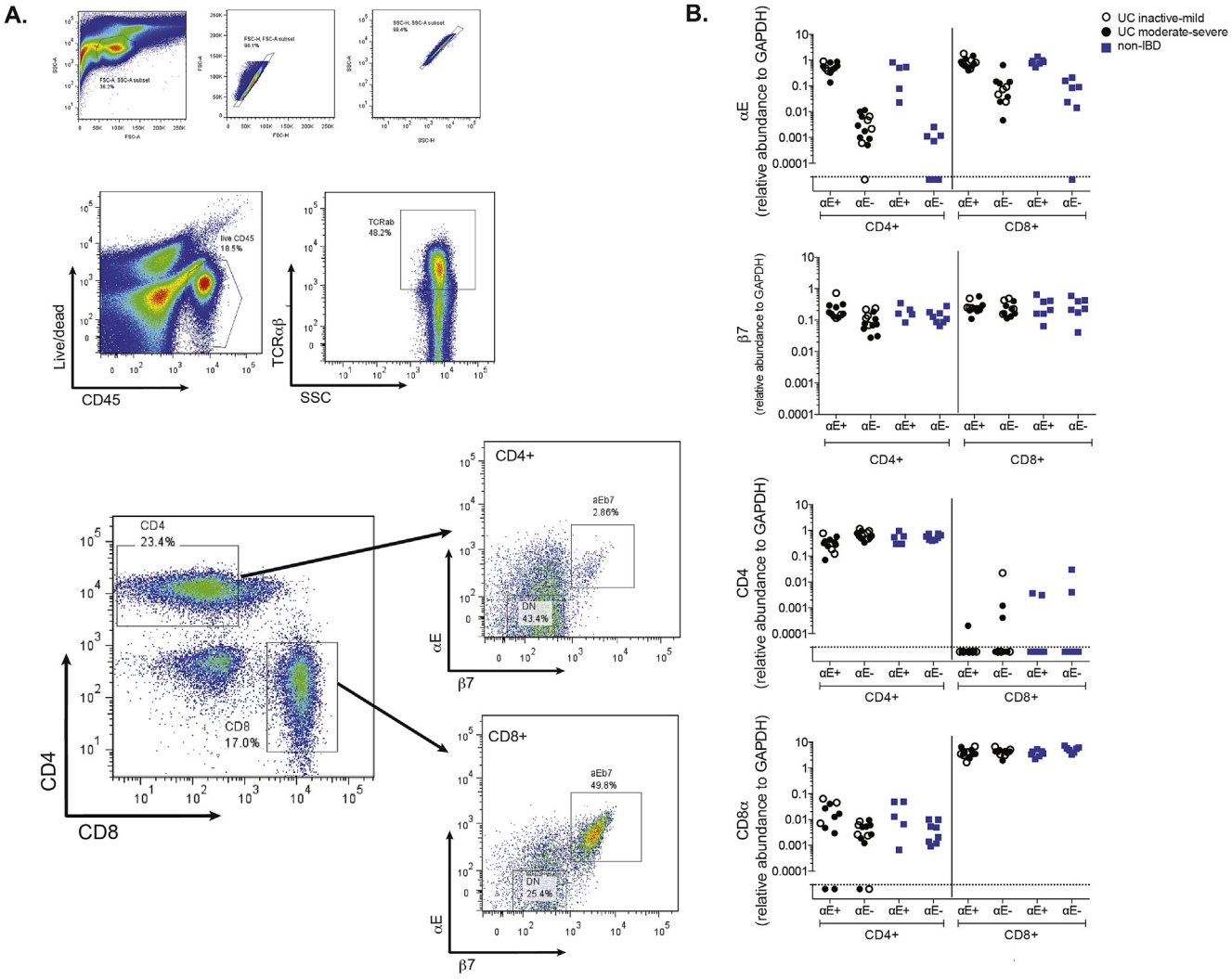

Supplementary Figure 3. Sort strategy and qPCR profiling of αE^+ and αE^- T cells. (*A*) Biopsies from UC patients and healthy controls enrolled in cohort 2 were sorted based on size and single cells (*top row*), then live $CD45^+$ $TCR\alpha\beta^+$ (*middle row*) were further sorted into $CD4^+\alpha E\beta7^+$ and $CD4^+\alpha E\beta7^-$ cell populations and $CD8^+\alpha E\beta7^+$ and $CD8^+\alpha E\beta7^-$ cell populations (*bottom row*). Healthy control is shown. (*B*) qPCR of sort purified cells for the sort parameters αE, $\beta7$, CD4, and CD8.

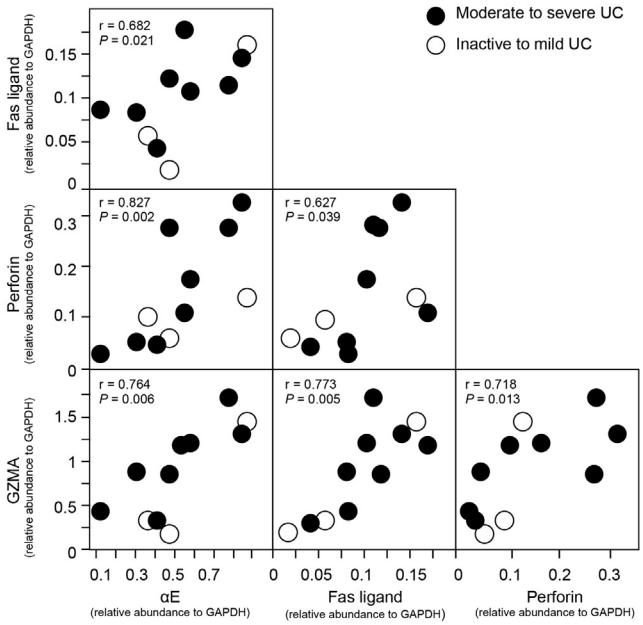

Supplementary Figure 4. Correlation of αE and effector molecule gene expression in flow cytometry sort-purified CD4$^{+}\alpha$E^{+} cells in UC patients. Sort-purified CD4$^{+}\alpha$E^{+} cells from cohort 2 were evaluated for gene expression of effector molecules. The correlation in gene expression between effector molecules perforin, Fas ligand with granzyme A, and αE in sort purified CD4$^{+}\alpha$E^{+} cells in UC patients is shown.

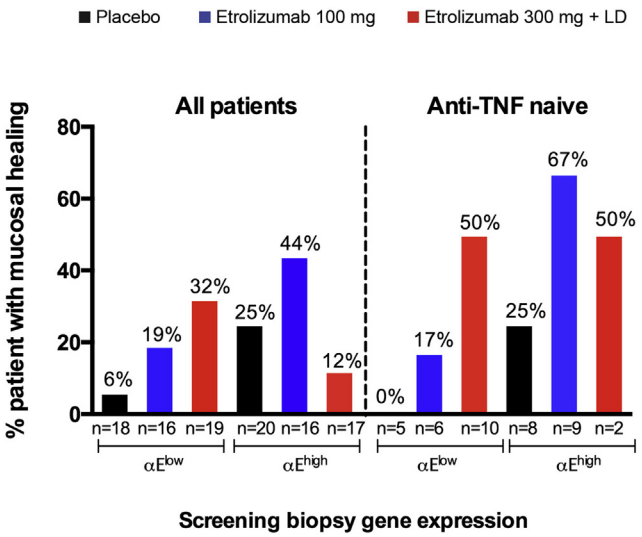

Supplementary Figure 5. Proportion of patients with mucosal healing by biomarker αE stratification. Baseline colonic biopsy qPCR median value was used as cutoff to categorize patients as αE^{high} (greater than or equal to median) or αE^{low} (less than median).

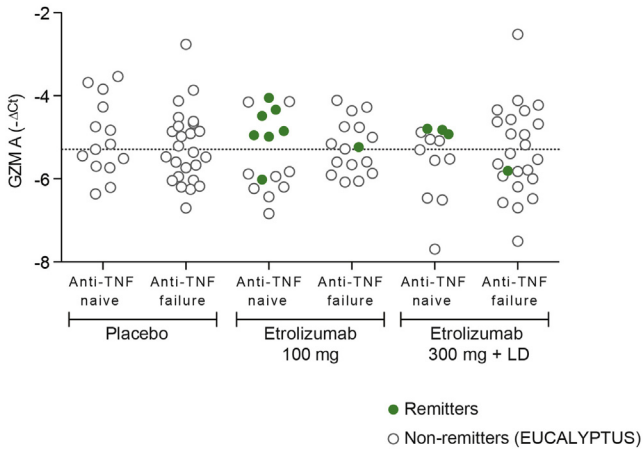

Supplementary Figure 6. Distribution of baseline colonic gene expression of granzyme A by dose group and anti-TNF status. Granzyme A gene expression relative to GAPDH expression in baseline colonic biopsies from cohort 1. The *dotted line* indicates the median.

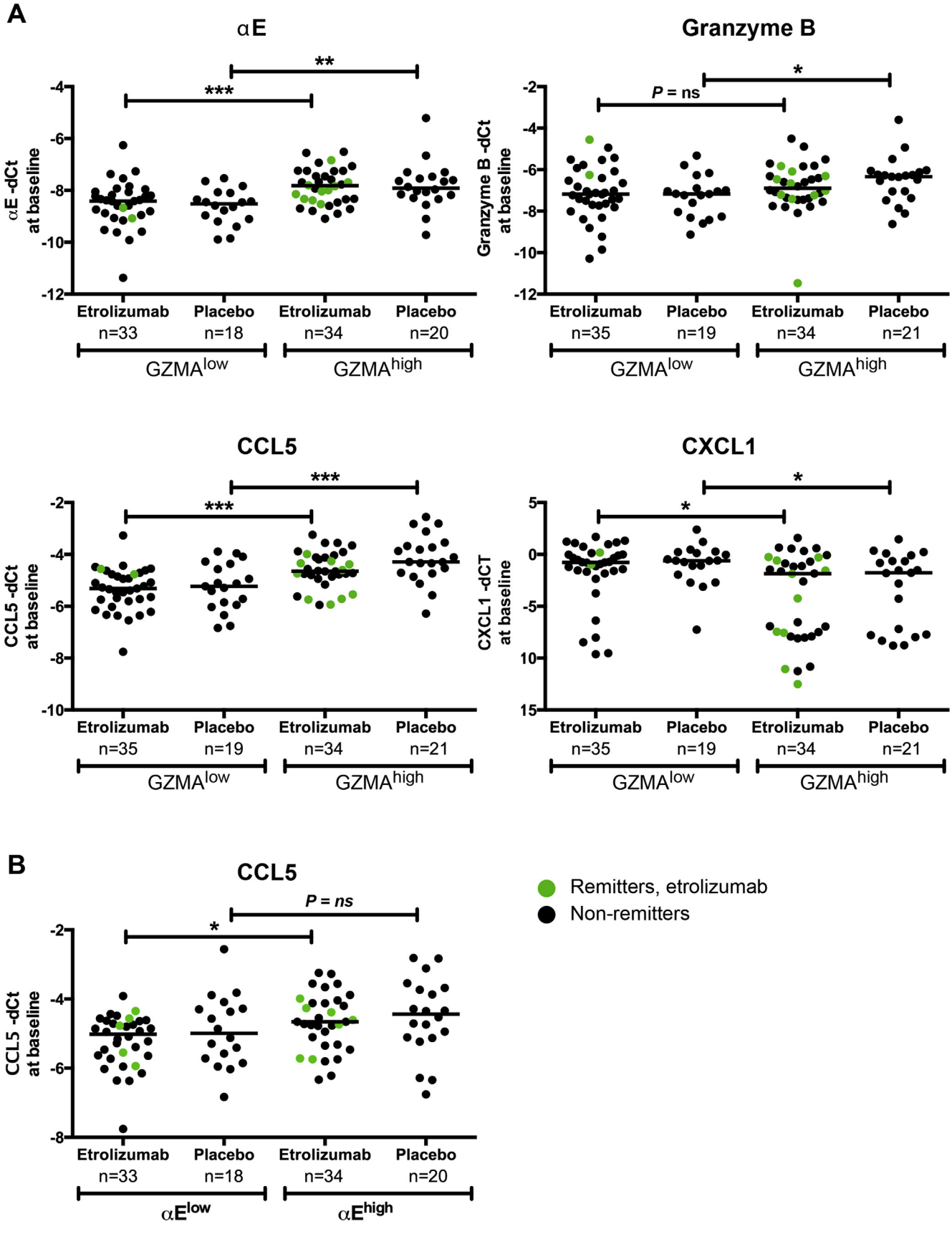
A
αE
αE -dCt at baseline
***
**
Etrolizumab n=33
Placebo n=18
Etrolizumab n=34
Placebo n=20
GZMA^low
GZMA^high
Granzyme B
Granzyme B -dCt at baseline
P = ns
*
Etrolizumab n=35
Placebo n=19
Etrolizumab n=34
Placebo n=21
CCL5
CCL5 -dCt at baseline
CXCL1
CXCL1 -dCT at baseline
B
CCL5
P = ns
αE^low
αE^high
Remitters, etrolizumab
Non-remitters

Supplementary Figure 7. Distribution of baseline gene expression of αE, granzyme B, CXCL1, and CCL5 by biomarker status and treatment group. Baseline colonic biopsy gene expression was assessed by qPCR in cohort 1. Baseline colonic biopsy qPCR median value was used as cutoff to categorize patients as granzyme A^{high} or αE^{high} (greater than or equal to median) or granzyme A^{low} or αE^{low} (less than median). (*A*) αE, granzyme B, CCL5, and CXCL1 gene expression relative to glyceraldehyde-3-phosphate dehydrogenase (phosphorylating) (GAPDH) expression in baseline colonic biopsy by granzyme A status. (*B*) CCL5 expression relative to GAPDH in baseline colonic biopsy by αE status. NS, not significant; *$P < .05$; **$P < .01$; ***$P < .001$.

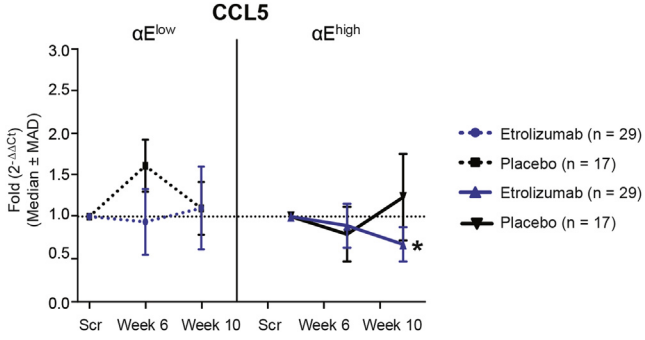

Supplementary Figure 8. Effect of etrolizumab on CCL5 colonic biopsy gene expression by αE stratification. Colonic biopsy gene expression was assessed by qPCR before and after treatment with etrolizumab or placebo in cohort 1. Baseline colonic biopsy qPCR median value was used as cutoff to categorize patients as αE^{high} (greater than or equal to median) or αE^{low} (less than median). Decreased CCL5 expression in colonic biopsy in αE^{high} patients treated with etrolizumab, but not αE^{low} patients relative to placebo was observed. Data presented as fold ($2^{-\Delta\Delta Ct}$) group median $\pm$ median absolute deviation. *P* values correspond to the comparison between etrolizumab and placebo. *$P < .05$ (vs placebo). SCR, screening.

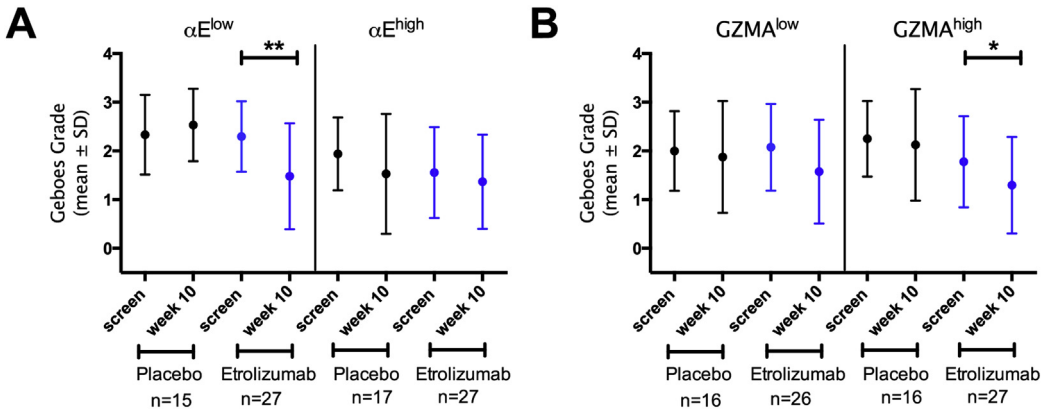

Supplementary Figure 9. Baseline and post-treatment histologic score by biomarker stratification. Histologic activity was evaluated using the modified Geboes score[30] for biopsies taken at the screening visit and week 10 in cohort 1. Baseline colonic biopsy qPCR median value was used as cutoff to categorize patients as granzyme A^{high} or αE^{high} (greater than or equal to median) or granzyme A^{low} or αE^{low} (less than median). Change in modified Geboes score before and after treatment with etrolizumab or placebo by baseline biopsy (*A*) αE or (*B*) granzyme A gene expression levels. $^{*}P < .05$; $^{**}P < .01$.

Supplementary Table 1. Curated Gene Lists of Sorted Cell Subsets

T cells	
Symbol	Gene name
CD3E	CD3e molecule, epsilon (CD3-TCR complex)
CTLA4	Cytotoxic T-lymphocyte-associated protein 4
CD8B	CD8b molecule
CD3D	CD3d molecule, delta (CD3-TCR complex)
CD3G	CD3g molecule, gamma (CD3-TCR complex)
ICOS	Inducible T-cell co-stimulator
DGKA	Diacylglycerol kinase, alpha 80 kDa
TRAT1	T cell receptor associated transmembrane adaptor 1
GPR15	G protein-coupled receptor 15
INPP4B	Inositol polyphosphate-4-phosphatase, type II, 105 kDa
ZBED2	zinc finger, BED-type containing 2
CAMK4	Calcium/calmodulin-dependent protein kinase IV
PIK3IP1	Phosphoinositide-3-kinase interacting protein 1
CD6	CD6 molecule
CD5	CD5 molecule
GZMK	Granzyme K (granzyme 3; tryptase II)
CXCR6	Chemokine (C-X-C motif) receptor 6
CDK1	Cyclin-dependent kinase 1
TCF7	Transcription factor 7 (T-cell specific, HMG-box)

Neutrophils	
Symbol	Gene name
MANSC1	MANSC domain containing 1
TNFRSF10C	Tumor necrosis factor receptor superfamily, member 10c, decoy without an intracellular domain
CXCR1	Chemokine (C-X-C motif) receptor 1
CXCR2	Chemokine (C-X-C motif) receptor 2
FFAR2	Free fatty acid receptor 2
PROK2	Prokineticin 2
CMTM2	CKLFlike MARVEL transmembrane domain containing 2
KRT23	Keratin 23 (histone deacetylase inducible)
FCGR3B	Fc fragment of IgG, low affinity IIIb, receptor (CD16b)
CCR3	Chemokine (C-C motif) receptor 3
CLC	Charcot-Leyden crystal protein
R3HDM4	R3H domain containing 4

Dendritic cells	
Symbol	Gene name
ADAM12	ADAM metallopeptidase domain 12
CCL17	Chemokine (C-C motif) ligand 17
CD1A	CD1a molecule
CD1B	CD1b molecule
CD1E	CD1e molecule
NR4A3	Nuclear receptor subfamily 4, group A, member 3
CXCL11	Chemokine (C-X-C motif) ligand 11
GPR157	G protein-coupled receptor 157
FSCN1	Fascin homolog 1, actin-bundling protein
SLCO5A1	Solute carrier organic anion transporter family, member 5A1
RAB30	RAB30, member RAS oncogene family
PDCD1LG2	Programmed cell death 1 ligand 2
USP18	Ubiquitin specific peptidase 18

Supplementary Table 1. Continued

Dendritic cells	
Symbol	Gene name
NUB1	Negative regulator of ubiquitin-like proteins 1
C5orf20	Chromosome 5 open reading frame 20
CLEC10A	C-type lectin domain family 10, member A
ARHGAP22	Rho GTPase activating protein 22

Monocytes	
Symbol	Gene name
CTSD	Cathepsin D
IL3RA	Interleukin 3 receptor
VCAN	Versican
PTX3	Pentraxin 3
SERPINB2	Serpin peptidase inhibitor
MMP19	Matrix metallopeptidase 19
CLEC5A	C-type lectin domain family 5
BHLHE41	Basic helix-loop-helix family
PLD3	Phospholipase D family
SLC31A1	Solute carrier family 31 (copper transporters)
ZEB2	Zinc finger E-box binding homeobox 2
TNFSF15	Tumor necrosis factor (ligand) superfamily
DFNA5	Deafness
KLF10	Kruppel-like factor 10
PID1	Phosphotyrosine interaction domain containing 1

B cells	
Symbol	Gene name
VPREB3	Pre-B lymphocyte 3
FCRL5	Fc receptor-like 5
MZB1	Marginal zone B and B1 cell-specific protein
PNOC	Prepronociceptin
CD19	CD19 molecule
CD79A	CD79a molecule, immunoglobulin-associated alpha
MS4A1	Membrane-spanning 4-domains, subfamily A, member 1
DTNB	Dystrobrevin, beta
TCL1A	T-cell leukemia/lymphoma 1A
TNFRSF17	Tumor necrosis factor receptor superfamily, member 17
FCRL2	Fc receptor-like 2
BLK	B lymphoid tyrosine kinase
FCRL1	Fc receptor-like 1
GNG7	Guanine nucleotide binding protein (G protein), gamma 7
SPIB	Spi-B transcription factor (Spi-1/PU.1 related)
RALGPS2	Ral GEF with PH domain and SH3 binding motif 2
FAM129C	Family with sequence similarity 129, member C
OSBPL10	Oxysterol binding protein-like 10
BANK1	B-cell scaffold protein with ankyrin repeats 1
KLHL14	Kelch-like 14 (Drosophila)
CPNE5	copine V
CD79B	CD79b molecule, immunoglobulin-associated beta
POU2AF1	POU class 2 associating factor 1
BLNK	B-cell linker
TNFRSF13C	Tumor necrosis factor receptor superfamily, member 13C

NOTE. Genes used for each of the leukocyte subsets in the gene-set enrichment analysis are listed.

Supplementary Table 2. Clinical Remission by Biomarker Subgroups

Anti−TNF-naïve[a]		
100-mg dose group	αE^{high}	αE^{low}
$GZMA^{high}$	86 (6/7)	0 (0/1)
$GZMA^{low}$	0 (0/2)	20 (1/5)
300 mg + LD dose group	αE^{high}	αE^{low}
$GZMA^{high}$	50 (1/2)	50 (2/4)
$GZMA^{low}$	No data	0 (0/6)
All patients[b]		
100-mg dose group	αE^{high}	αE^{low}
$GZMA^{high}$	55 (6/11)	17 (1/6)
$GZMA^{low}$	0 (0/5)	13 (1/8)
300 mg + LD dose group	αE^{high}	αE^{low}
$GZMA^{high}$	9 (1/11)	33 (2/6)
$GZMA^{low}$	0 (0/6)	8 (1/13)

NOTE. Gene expression of baseline colonic biopsies using qPCR median as cutoff was used to categorize patients as biomarker high and low.
[a]Values shown are percentage of anti−TNF-naïve etrolizumab-treated patients in remission at week 10 (n in remission/total).
[b]Values shown are percentage of etrolizumab-treated patients in remission at week 10 (n in remission/total).

Supplementary Table 3. Baseline Characteristics by Biomarker Subgroups

	$GZMA^{low}$ (n = 54)	$GZMA^{high}$ (n = 55)	αE^{low} (n = 53)	αE^{high} (n = 53)
Age, *y*, mean ± SD	37 ± 14	43 ± 13[a]	39 ± 14	41 ± 13
Male, n (%)	34 (63)	30 (55)	32 (60)	30 (57)
Duration of UC, *y*, mean (range)	9.1 (0.3−30.1)	9.3 (0.5−40.9)	5.6 (0.3−30)	8 (1−41)
Concomitant medication use, n (%)				
Corticosteroids	22 (41)	25 (46)	24 (45)	23 (43)
Immunosuppressants	30 (56)	14 (25)[b]	24 (45)	19 (36)
Previous anti-TNF use	34 (63)	33 (60)	32 (60)	34 (64)
Previous anti-TNF failure	33 (61)	30 (55)	30 (57)	32 (60)
Disease extent, n (%)				
Left-sided colitis	23 (43)	17 (31)	22 (42)	17 (32)
Pancolitis/extensive disease	16 (30)	26 (48)	18 (34)	22 (42)
Rectosigmoid	14 (26)	12 (22)	12 (23)	14 (26)
Other	1 (2)	0	1 (2)	0
Disease activity, mean ± SD				
Mayo Clinic score	9.2 ± 1.5	9.5 ± 1.5	9.7 ± 1.5	9.1 ± 1.4
Rectal bleeding	1.8 ± 0.6	1.9 ± 0.7	1.8 ± 0.7	1.7 ± 0.6
Stool frequency	2.5 ± 0.7	2.6 ± 0.6	2.7 ± 0.7	2.5 ± 0.7
Endoscopy	2.6 ± 0.5	2.6 ± 0.5	2.8 ± 0.4	2.5 ± 0.5[c]
Physician global assessment	2.3 ± 0.6	2.4 ± 0.5	2.4 ± 0.6	2.3 ± 0.5
Modified Geboes score, mean ± SD (n)	2.1 ± 0.8 (47)	1.9 ± 0.9 (48)	2.3 ± 0.8 (46)	1.7 ± 0.9[c] (46)

NOTE. Gene expression of baseline colonic biopsies using qPCR median as cutoff was used to categorize patients as biomarker high and low.
[a]$P < .05$ vs $GZMA^{low}$.
[b]$P < .01$ vs $GZMA^{low}$.
[c]$P < .01$ vs αE^{low}.